

Materials and Process Activities for NASA's Composite Crew Module

Daniel L. Polis
National Aeronautics and Space Administration
Goddard Space Flight Center
Greenbelt, MD 20771

ABSTRACT

In January 2007, the NASA Administrator and Associate Administrator for the Exploration Systems Mission Directorate chartered the NASA Engineering and Safety Center (NESC) to design, build, and test a full-scale Composite Crew Module (CCM). The overall goal of the CCM project was to develop a team from the NASA family with hands-on experience in composite design, manufacturing, and testing in anticipation of future space exploration systems being made of composite materials. The CCM project was planned to run concurrently with the Orion project's baseline metallic design within the Constellation Program so that features could be compared and discussed without inducing risk to the overall Program.

The materials and process activities were prioritized based on a rapid prototype approach. This approach focused developmental activities on design details with greater risk and uncertainty, such as out-of-autoclave joining, over some of the more traditional lamina and laminate building block levels. While process development and associated building block testing were performed, several anomalies were still observed at the full-scale level due to interactions between process robustness and manufacturing scale-up.

This paper describes the process anomalies that were encountered during the CCM development and the subsequent root cause investigations that led to the final design solutions. These investigations highlight the importance of full-scale developmental work early in the schedule of a complex composite design/build project.

1. INTRODUCTION

1.1 Process Development and Validation

The CCM structure was comprised of design details including composite laminate, composite sandwich, metal-composite bonded joints, metal-composite bolted joints, composite-composite splice joints, and composite-composite 3D woven joints. Complete details regarding the CCM project, design, analysis, materials and processes, manufacturing and performance can be found in Reference 1 thru 7.

Given the complexity of the structure and associated processes to produce it, baseline processes were established from the existing knowledgebase on the CCM team, which included several NASA Centers, Alliant Techsystems, Inc.(ATK), Cytec, Lockheed Martin (LM), and Northrop Grumman Corporation (NGC) team members.

This paper is declared a work of the U.S. Government and is not subject to copyright protection in the United States.

While these baseline processes were initially used in the fabrication of test coupons and test elements, process development was an ongoing activity. This process evolution was driven by design changes, manufacturing constraints, or to solve process issues (anomalies). One such process that underwent significant evolution during the life of the project was the process used to produce the sandwich shells. Figure 1 shows a schematic cut away view of the CCM pressure shell, with excerpts highlighting a constant thickness and tapered cross sections of the composite sandwich and sandwich to solid laminate transition, respectively.

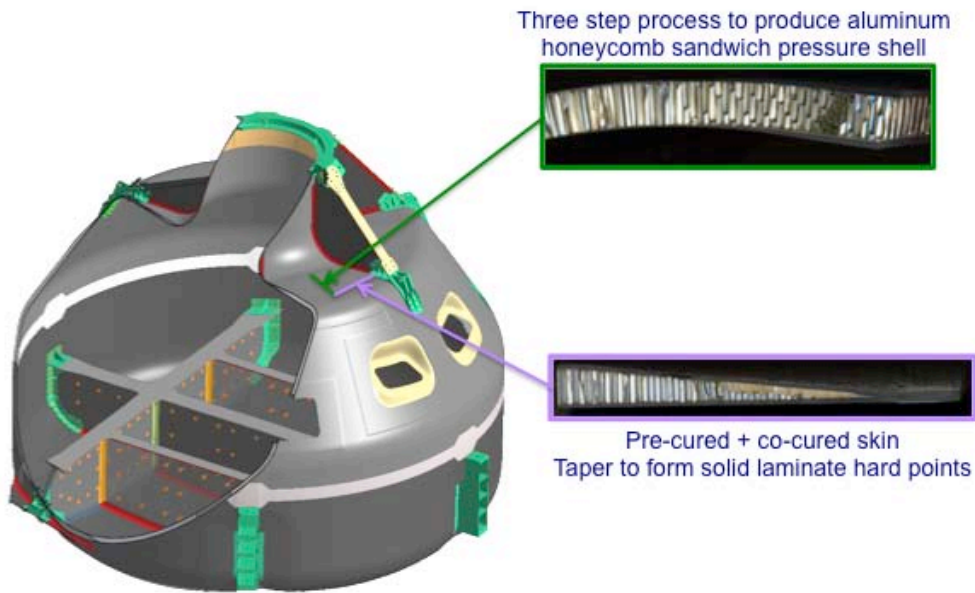


Figure 1: Schematic cut-away view with showing constant thickness and tapered sandwich cross sections.

The process used to produce the sandwich shells was a 3-step process (Type I process) consisting of the following:

1. Producing a pre-cured skin (inner mold line, IML, skin)
2. Tacking or bonding the core to the pre-cured skin
3. Co-curing the second skin (outer mold line, OML, skin) on top of the core to complete the sandwich and solid laminate.

A 3-step process was chosen for the upper pressure shell (UPS) and lower pressure shell (LPS) because the team felt it provided the best combination of high performance and low manufacturing risk. Alternative approaches are processes that use two co-cured skins, two pre-cured skins, or combine steps 2 and 3 from above. While a three-step process was ultimately implemented with success, both from a manufacturing and performance perspective, the process required significant development due to various anomalies that arose during the development cycle. Figure 2 contains a flow chart describing the evolution of this process. This flow chart highlights various process changes. This paper documents this process evolution, including anomalies, process studies, and corrective actions.

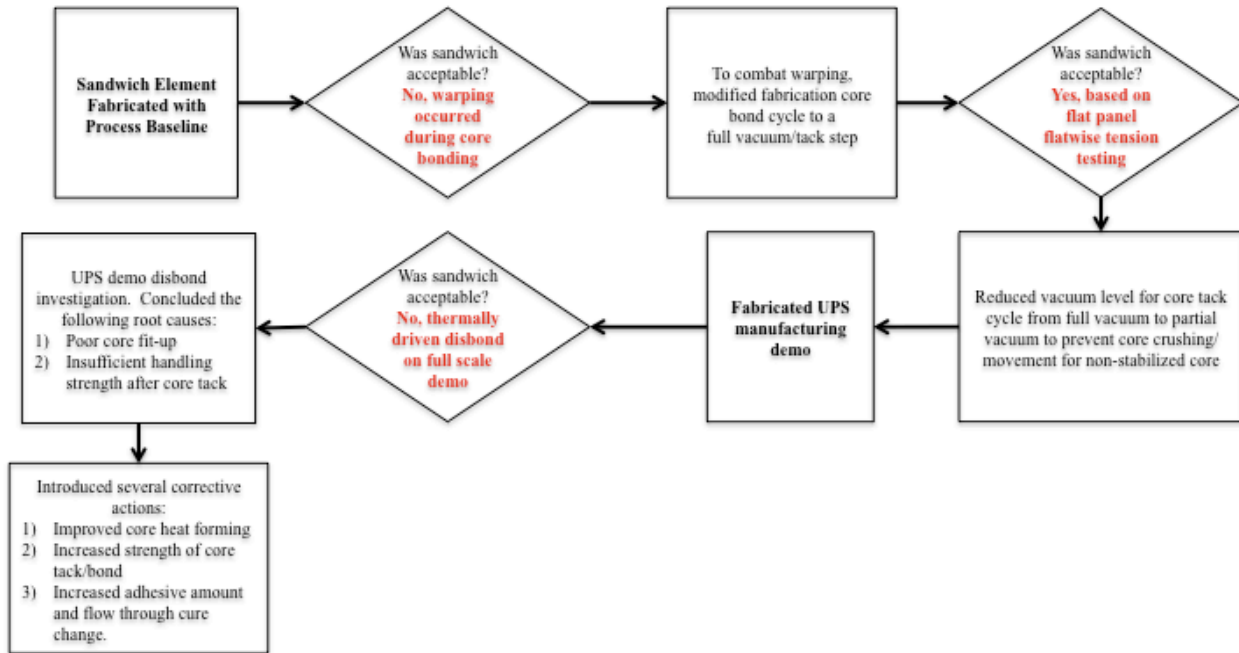


Figure 2: Flow Chart showing process development drivers for 3-step sandwich cure.

2. FLAT PANEL WARPING

The baseline core bonding cycle for sandwich shell fabrication process was a core bonding cycle to 177 °C (350 °F). The cycle achieved full core bonding strength prior to adding the co-cured outer skin. However, during flat panel element manufacturing, considerable warpage was observed due to the asymmetric configuration at the intermediate core bonding stage. Laying the OML on these warped panels and performing debulk steps proved difficult. Therefore, the core-bonding step was modified to reduce the warping.

Based on the work by Curiel and Furlund [Reference 8], a two-step cure process for the core-IML bond was introduced. The first step was called the tack step and took the core-IML assembly to 121°C (250 °F). The assembly was then brought to room temperature for OML layup. At this point the film adhesive had flowed, gelled, but not achieved full strength. The subsequent cure of the OML would impart the full cure strength to the core-IML bond. It is important to note that for flat panel fabrication, this approach was successful in eliminating warping.

This process change was validated using flatwise tension testing, in accordance with Reference 9. The test matrix, summarized in Table 1, as performed with aluminum facesheets and 5056-1/4-7.9-PAA core using 244 gsm (0.05 psf) FM[®] 300M. Because the cell size is different than the CCM cells (strength depends on the cell wall length per unit area), the results should only be used for relative comparison.

Table 1: Core Bonding Evaluation Matrix

	Full Vacuum 1.01 e5 Pa (14.6 psi) differential	Partial Vacuum 3.38 e4 Pa (4.9 psi) differential	Autoclave Pressure 2.76e5 Pa (40 psi) differential
1-step process (straight ramp to 177 °C)	A: Entire cycle at full vacuum/no autoclave	B: Entire cycle at partial vacuum/no autoclave	C: Entire cycle at no vacuum/2.76e5 Pa autoclave
2-step process (121 °C tack; cool to RT; 177 °C final)	D: Entire cycle at full vacuum/no autoclave	E: Entire cycle at partial vacuum/no autoclave	F: Tack cycle at partial vacuum/no autoclave followed by cool to RT and ramp to 177 °C under no vacuum/2.76e5 Pa autoclave

Figure 3 shows the flatwise strength from this test matrix. This matrix and test data is referenced in subsequent sections, but here a one-step process is compared with a two-step process. It is apparent from the flat aluminum sandwich results that there is no difference using the one-step or two-step process, from an end product strength perspective. While these panels do not contain the same residual stress as ones made with a composite skin, they address the concern of good filleting, which is strongly affected by the cure profile, due to flow characteristics during cure.

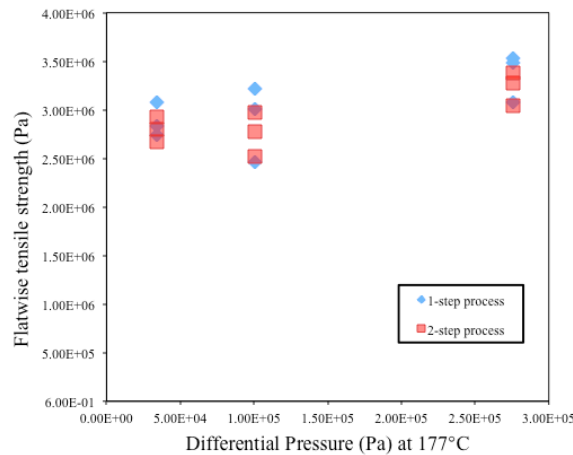


Figure 3. Flatwise Tensile Strength versus Differential Pressure

A two-step process with full vacuum, 1.01e5 Pa (14.6 psi) differential pressure, was subsequently used for all of the sandwich test elements. Witness panels accompanied the fabrication of the test elements and were used for flatwise tensile strength validation. Figure 4 compares the witness panel results before and after the change from a one-step to a two-step process. In addition, Figure 4 shows witness results from a panel made with a Type III process, which is the CCM process for bonding two pre-cured skins to honeycomb using 2.76±0.35e5 Pa (40±5 psi) autoclave pressure. All of these witness panels show comparable results (within 10 percent) of the reference data from Cytac using comparable core.

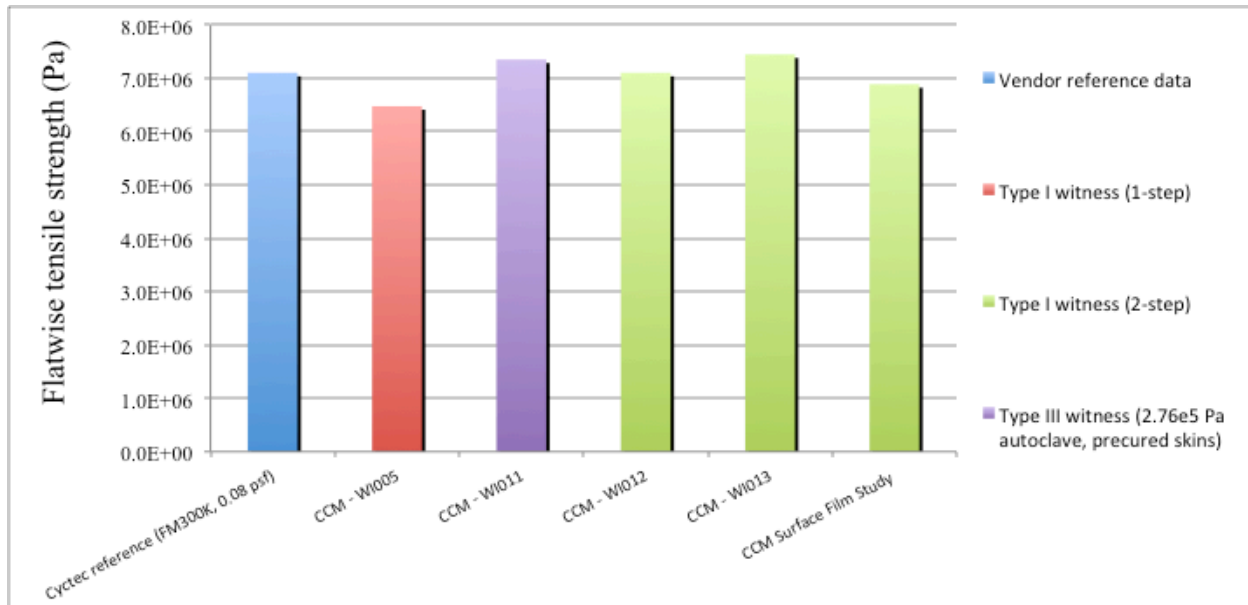


Figure 4. Flatwise Tensile Strength Process Comparison

The element tests and accompanying witness panels gave the team confidence that the core bonding process was acceptable. As mentioned in the following section, none of this testing factored in the geometric complexity, such as ply drops and core fit-up. In addition, the team did not consider the handling strength after the tack step.

3. VACUUM LEVEL REDUCTION

As the team transitioned from element testing to the UPS full-scale demonstration article, several complexities were added to the manufacturing and associated processes. One of these was the fact that the core needed to be heat formed on the tool, in contrast to flat sandwich panels. This was recommended by the core vendor to provide a better core fit-up. It was recommended that this be done at reduced vacuum levels, 3.38×10^4 Pa (4.9 psi), since the core was not stabilized to prevent any edges crushing or movement. Because this was the differential pressure that was used to do the core forming, it was also that used on the core impression film. Finally, this vacuum reduction was adopted for the core tack cycle. This reduction in differential pressure can be examined by comparing cells A, B, D and E in Table 1 and the results shown in Figure 3. The partial vacuum (3.38×10^4 Pa) data and full vacuum (1.01×10^5 Pa) data are statistically indistinguishable.

4. BOND ANOMALY OBSERVED IN THE UPS

The UPS manufacturing demonstration article was manufactured using a 3-step process, in which the core tack step was done at partial vacuum and 121°C using FM[®] 300. After the core was tacked to the IML, the OML skin was laid-up and cured successfully. A through

transmission ultrasonic inspection was performed on the demonstration article and indicated that the sandwich was of good quality.

Subsequent to the OML cure and inspection, an IML doubler was laid-up and cured at 177 °C on the bottom edge of the shell. Following this IML doubler cure cycle, a disbond was observed between the IML skin and core. The disbond was located in the hatch area, as shown in Figure 5. This hatch zone was originally thought to be a unique detail, because it had been designed with only one ply, since it would subsequently be cut out for frame installation. The intent was to reduce distortion upon removal of the hatch sandwich.

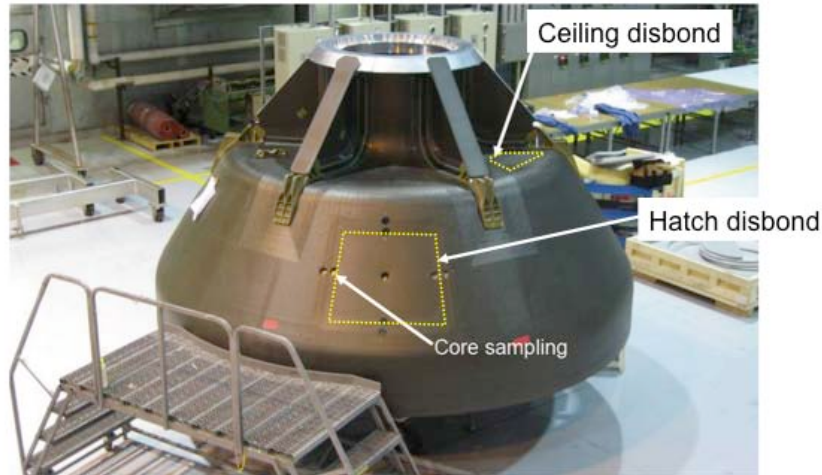


Figure 5: UPS Manufacturing demonstration article disbond location

This presented two notable distinctions for the hatch area: increased potential for water intrusion during the ultrasonic inspection and a rapid ply drop zone (24 plies dropping to 1 ply), that was not present in other locations on the shell. Several 50.8 mm diameter samples were cored from the hatch area, both inside and outside the disbond perimeter, as shown from the IML view in Figure 6.

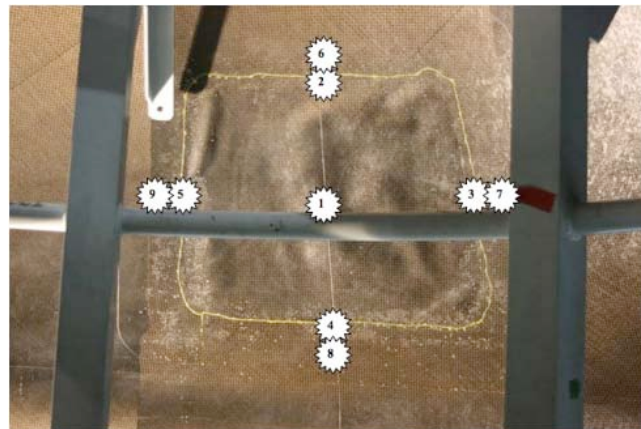


Figure 6: UPS Demo IML Hatch Disbond and Sample Extraction Locations

Figure 7 shows sampe #3. It is clear from this and other extractions that the core was bridged, because the hexagonal cells did not make full impressions on the film adhesive. Zones where this is evident are indicated by the dotted lines in the figure and correspond to orientations commensurate with rapid ply drops. Figure 8 shows the cross-sectional view from sample #5. This shows the core sitting on top of the film adhesive in an area where the plies drop rather rapidly.

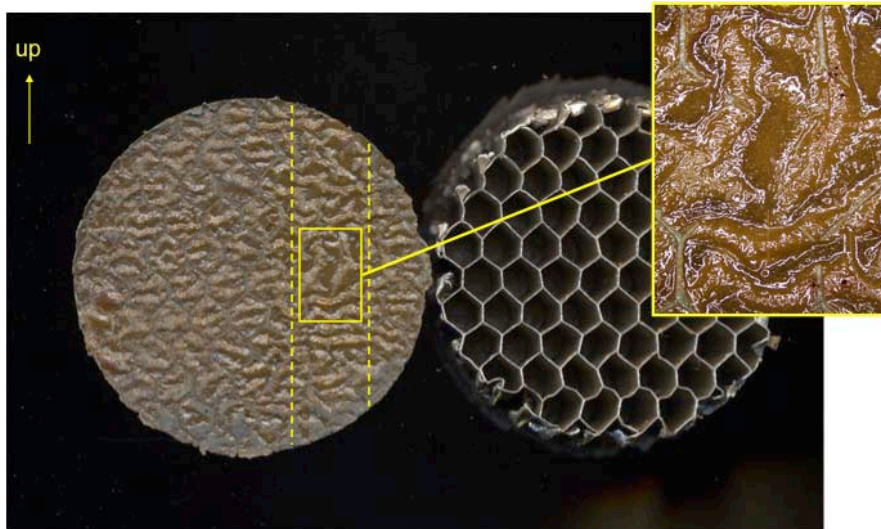


Figure 7: Hatch Extraction Sample #3, IML bondline

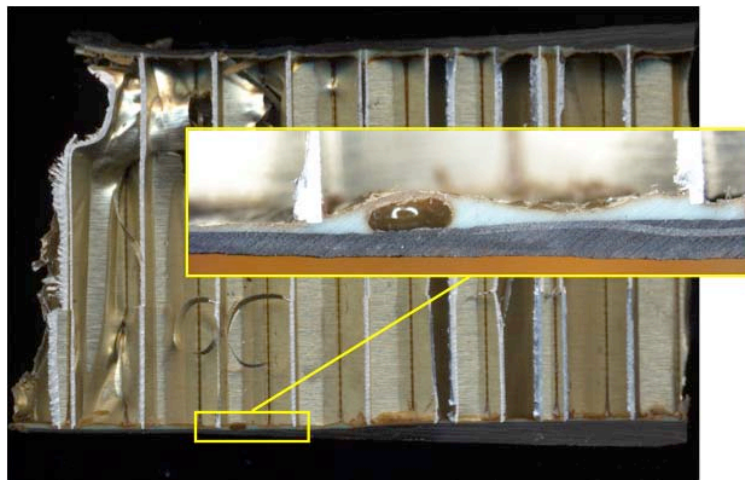


Figure 8: Hatch Extraction Sample #5, inset showing IML bondline

Because this initial hatch disbond was thought to be caused, in part, by the unique hatch geometry and layup, the manufacturing of the UPS demonstration article proceeded following the core sampling from the hatch area. Subsequent to the disbond in the hatch, the UPS was

taken through another heat cycle to bond six gussets to the tunnel-ceiling area. During cool down, at ~30 °C, an audible sound was heard. Subsequent visual evaluation revealed an IML skin to core disbond in the ceiling (bay C), which is highlighted in Figure 5. This observation initiated a more extensive anomaly investigation process, which is detailed in the following section.

5. CORE BOND INVESTIGATION

5.1 Overview

It is instructive to point out that for any bond failure there is both a stress component and a strength component. In other words, for failure to occur the bond stress exceeded the bond strength. However, during the investigation the team did not explore the residual thermal stress, or other mechanical stress components, based on the ability to readily model them accurately (requires detailed solid model) and the ability to alter them significantly. The team's focus was therefore on causes that could lead to strength degradation.

5.2 Flatwise Tension Test Matrix

One of the primary tools for evaluating cause and effect was flatwise tensile testing. This test probes the strength of the core-to-facesheet bonds and could be applied to the witness panels, UPS demo article, and sensitivity studies designed at determining root cause of the disbond.

Reference 9 prescribes a specimen (round or square) which has a minimum area of 2600 mm². However, the team chose a custom geometry, which used a 50.8 mm diameter specimen bonded to 38.1 mm diameter blocks. This was done for several reasons: facilitated sample removal from complex articles, provided relief on sample edge condition, and increased the number of samples that could be extracted from small panels. This configuration is shown in Figure 9 and will be referred to as the overhang coupon.

Due to the nonstandard coupon, a finite element model was built of the configuration and examined with various facesheet thicknesses to examine the extent of load transfer in the overhang region. For a 4 ply skin (0.81 mm thick), the load transfer in the overhang region is small, leaving most of the facesheet-to-core bondline at stresses similar to a specimen without an overhang. In contrast, a 16 ply skin (3.25 mm thick) shows considerable load transfer in the overhang portion of the specimen, such that the entire 50.8 mm diameter specimen shows nearly uniform stress at the facesheet-to-core bondline. These present the two extreme examples: thin skin showing nearly uniform stress over a 38.1 mm diameter zone versus thick skin showing uniform stress of the 50.8 mm diameter zone. For the sake of reporting, the team used the 38.1 mm diameter to report failure stresses, because the entire sensitivity study reported in this section use thin gage skins. However, these stresses should be only compared for identical facesheet/core combinations.

A sensitivity study was designed to look at the effect of pressure differential, tack temperature, core contamination, core heat forming, and film adhesive weight. In addition some specimens were made by bonding over a 2-ply drop-off (step) to examine the ability to accommodate such a geometric feature, which may be encountered on the full-scale article. The fabrication of the test specimens is shown in Figure 10, highlighting the position of the ply drops. The detailed test

matrix is provided in Table 2, where the items highlighted in red represent deviations from the UPS manufacturing demonstration article process, which is given in column 1 of the table. Each column contains samples with and without ply drops, per Figure 10. All the reported failure results correspond to IML-to-core failure stresses.



Figure 9: Flatwise Tension Geometry used for Disbond Investigation

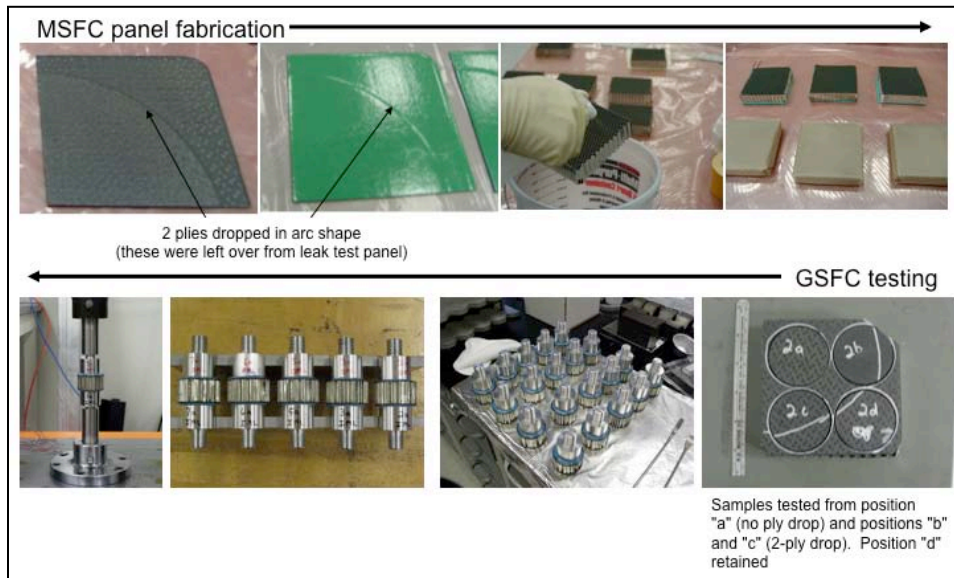


Figure 10: Flatwise Tension Fabrication Process Showing Ply Drop Position

The test matrix results are summarized in a box plot given in Figure 11. The most notable observation is that UPS baseline has the lowest mean and largest variability. However, it is instructive to dissect the main effects and interactions responsible for this response. Figures Figure 12 through Figure 15 examine various subsets of the test matrix.

Table 2: Flatwise Tension test matrix

Sample ID	1 (Baseline)	2	3	4	5	6	7	8	9	10	11	12
Core Contamination	No	No	No	No	Yes	No	No	No	No	No	No	No
350°F core forming	Yes	Yes	Yes	Yes	Yes	No	Yes	Yes	Yes	Yes	Yes	Yes
Core Contamination	No	No	No	No	No	No	No	No	No	No	Yes	No
Adhesive wt (gsm)	244	244	244	244	244	244	244	488	390.4	390.4	244	780.8
Adhesive type	FM300M	FM300M	FM300M	FM300M	FM300M	FM300M	FM300M	2 layers FM300M	FM300M + FM300U	FM300K	FM300M	2 layers FM300K
Vacuum (Pa)	-3.45E+04	-9.65E+04	-9.65E+04	-9.65E+04	-9.65E+04	-9.65E+04	0.00E+00	-9.65E+04	-9.65E+04	-9.65E+04	-9.65E+04	-9.65E+04
Autoclave (Pa)	0.00E+00	0.00E+00	0.00E+00	0.00E+00	0.00E+00	0.00E+00	2.76E+05	0.00E+00	0.00E+00	0.00E+00	0.00E+00	0.00E+00
1st ramp rate (°C/min)	0.56	0.56	0.56	0.56	0.56	0.56	0.56	0.56	0.56	0.56	0.56	0.56
1st hold temp (°C)	82	82	82	177	82	82	82	82	82	82	82	82
2nd ramp rate (°C/min)	0.56	0.56	0.56	N/A	0.56	0.56	0.56	0.56	0.56	0.56	0.56	0.56
2nd hold temp (°C)	121	121	149	N/A	121	121	121	121	121	121	121	121

First, the team examined the effect of film adhesive weight on the flatwise-tensile strength at a fixed differential pressure of 1.01×10^5 Pa (full vacuum). This result is summarized in a box plot in Figure 12. The results suggest that 244 gsm film is insufficient to achieve full strength, but 390 gsm or higher film weights are sufficient and indistinguishable. The UPS manufacturing demonstration article was built using 244 gsm film adhesive on both IML and OML skins. When these results were broken down even further, examining the interaction between film weight and the ability to accommodate ply drops, the team saw a more dramatic effect. Specifically, Figure Figure 13 shows this interaction plot. One can see that the thicker film adhesives (≥ 390 gsm) are unaffected by the ply drop, whereas the 244 gsm film shows a significant decrease in strength.

Next the team examined the effect of differential pressure on the flatwise-tensile strength at a fixed film weight (244 gsm). This result is summarized in a box plot in Figure 14. The results suggest that 3.38×10^4 Pa (partial vacuum) is not able to achieve full strength, but 1.01×10^5 Pa (full vacuum) or 2.76×10^5 Pa autoclave pressure are significantly stronger and indistinguishable from one another. The UPS demonstratin article was built using $\sim 3.38 \times 10^4$ Pa for the core-IML tack. The same conclusion is evident when the team broke the results down in an interaction diagram, as shown in Figure 15. This interaction plot shows nearly parallel lines in both plots, which indicates the effects are similar. In other words, regardless of pressure, the 2-ply drop decreases the measured flatwise strength.

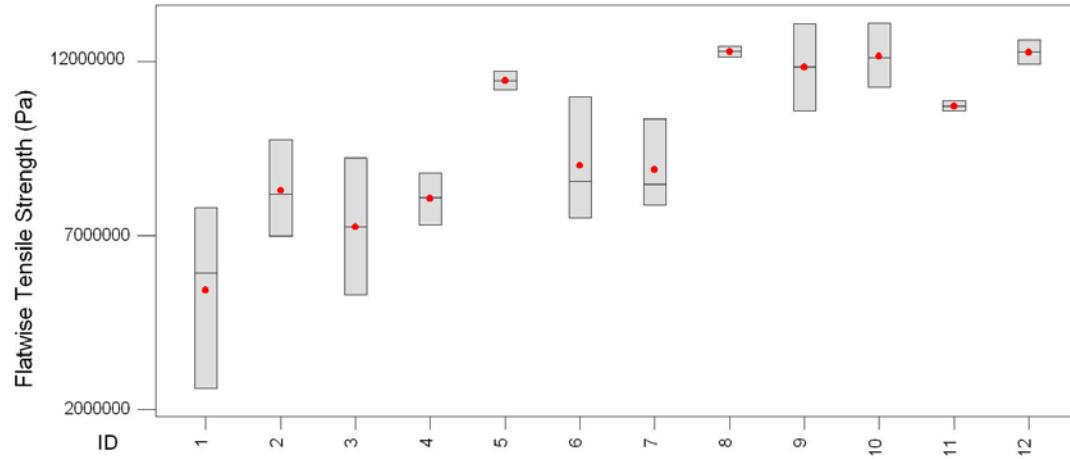


Figure 11: Box Plot Summarizing Flatwise Tension Strength for IML Disbond Investigation (red dots indicate mean values)

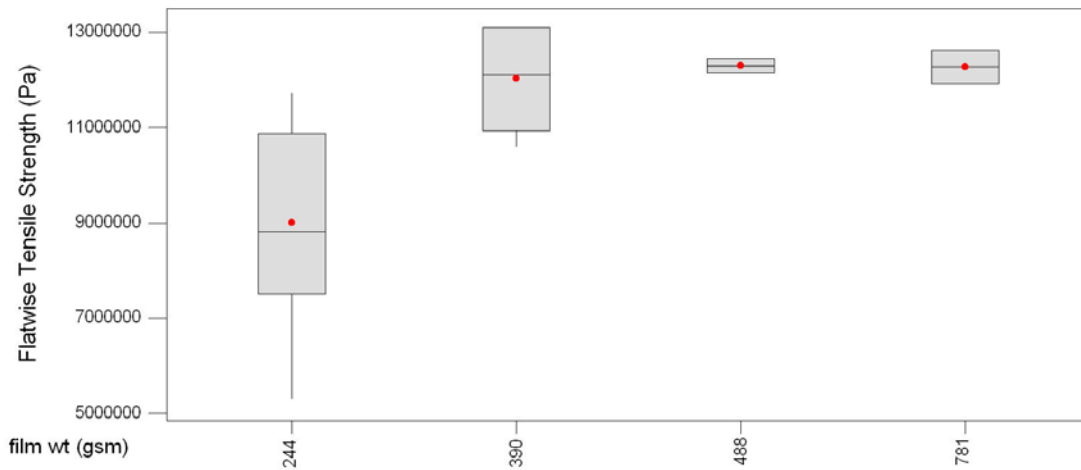


Figure 12: Box Plot of Flatwise Tension Strength at a Differential Pressure = 1.01×10^5 Pa (red dots indicate mean values)

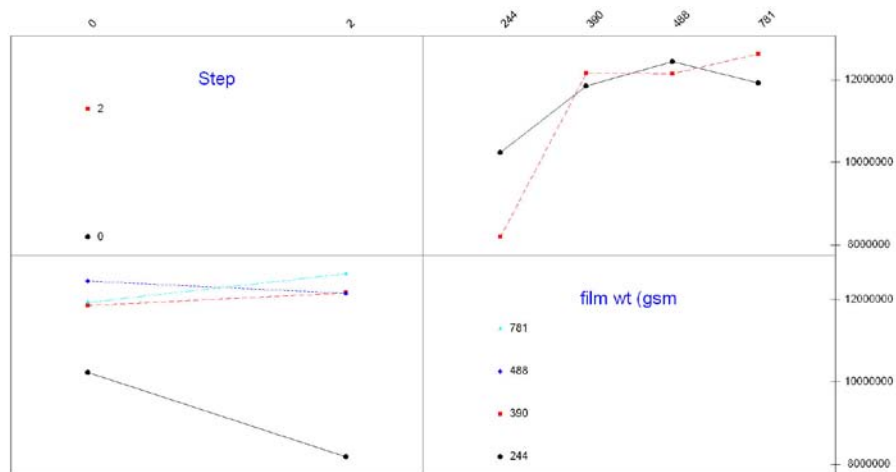


Figure 13: Interaction Plot of Flatwise Tension Strength at a Differential Pressure = 1.01e5 Pa

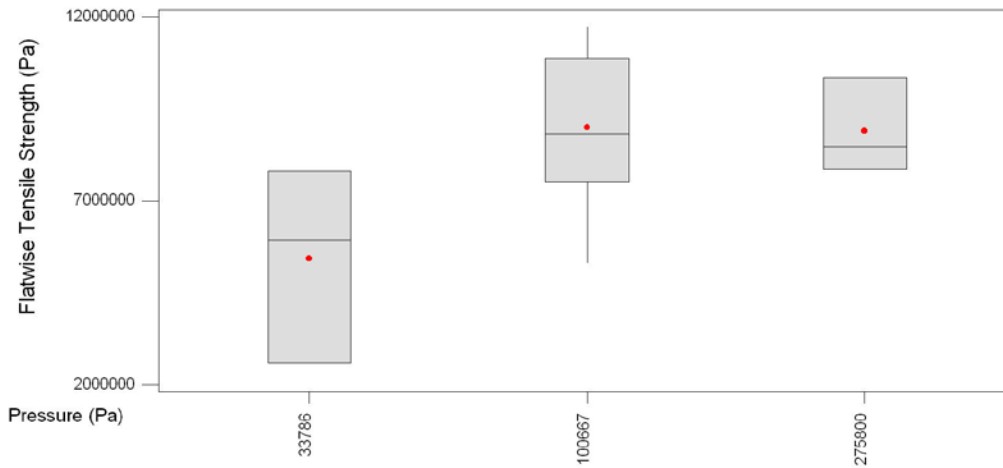


Figure 14: Box Plot of Flatwise Tension Strength for Film Adhesive Weights = 244 gsm (red dots indicate mean values)

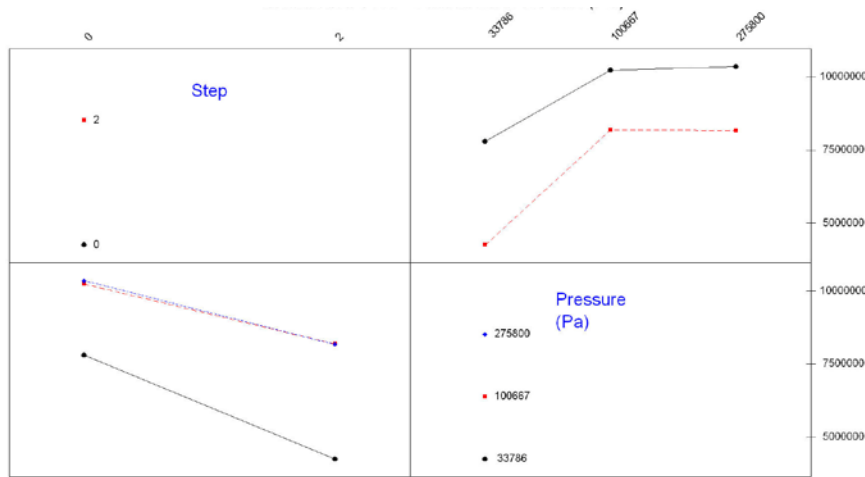


Figure 15: Interaction Plot of Flatwise Tension Strength for Film Adhesive Weights = 244 gsm

Several conclusions can be drawn from the flatwise-tensile strength portion of the investigation. The baseline test configuration reproduced the low IML-core bond strength. The baseline configuration of partial vacuum (3.38e4 Pa differential pressure) and 244 gsm film adhesive, coupled with a 2-ply geometric offset produced one coupon strength at 2.54e6 Pa, 50 percent of the next lowest test value in the entire test matrix. At a differential pressure of 1.01e5 Pa or higher, increasing the film weight to 390 gsm eliminates the detrimental effects of the 2-ply geometric offset, observed in the baseline. While increasing the differential pressure above 1.01e5 Pa did not show improved performance on these flat panels, it was anticipated that it could only help on complex geometry.

5.3 Filleting and Core Fit-up

Samples were extracted from each of the four windows on the UPS and cross-sectioned to examine the IML-core bond quality. Representative photomicrographs are shown in Figure 16. The main anomaly observed on the IML-core side is that the cells walls were far away from the laminate. This core to IML gap was measured on samples extracted from the UPS and samples taken from the flat witness panels made during the element-testing phase. The average gap was 0.12 mm for the UPS around the hatch versus 0.05 mm for the development panels. This UPS gap is more than half the nominal film adhesive thickness (244 gsm film adhesive has a nominal thickness of 0.20 mm). In contrast, the UPS flat witness panel had a similar core to IML gap as the previous witness panels. These observations point to an insufficient core fit-up for the given adhesive and pressure combination on a complex geometry.



Figure 16: Fillet Quality from Samples Extracted from the Four Windows

5.4 Core Bond Anomaly Investigation – Rheology

Although the previous section indicated that fillet quality was reasonable when the core was in good contact with the IML, it is instructive to examine the rheology to understand the sensitivity to cure parameters. A comparison of the rheology of FM[®] 300M film adhesive during a 1.9 °C/min ramp to 121 °C versus 177 °C. The main takeaway is that by using an intermediate tack step (121 °C) versus a full cure (177 °C), the minimum viscosity during filleting is 104.4 Pa*s versus 85.0 Pa*s, more than a 20 percent increase.

The difference between a 0.55 °C/min ramp rate versus 2.8 °C/min ramp rate to 121 °C was also examined. Note that they contain an intermediate hold temperature of 82 °C, per the tack cycle used on the UPS demonstration article. This ramp rate effect was found to increase the minimum viscosity from 87.2 Pa*s to 127.3 Pa*s for the slower ramp rate. It is also worth noting that while the lower limit on the cure specification was 0.55 °C/min, the actual ramp rate violated the specification, and was only ramped at 0.35 °C/min.

6. DISCUSSION: CAUSE AND CORRECTIVE ACTIONS

In the previous sections, the team highlighted some of the results from the anomaly investigation into the UPS core-IML disbond. This section summarizes relevant observations and corrective actions made during the investigation.

Core fit-up observations: A direct observation made on the UPS demonstration article was the fact that the core was not always in intimate contact with the shell. This was shown in photomicrographs extracted from the hatch area, Figure 8, and the four window cutouts, Figure 16. In addition, the flatwise tension test matrix demonstrated that with the reduced vacuum level (3.38×10^4 Pa differential pressure) and light weight film adhesive (244 gsm), poor core fit-up could not be overcome, as simulated with a 2-ply drop.

Core fit-up corrective actions: In order to overcome the issue of poor core-fit up, several corrective actions were put in place for the manufacturing of the CCM test article. The first was to heat form the core on top of the IML skin rather than on the tool. The team attempted to heat form over the pad-up areas. In addition, the film adhesive weight was increased from 244 gsm to 390 gsm for bonding pre-cured skins, which appeared to be the transition in performance, even at 1.01×10^5 Pa differential pressure. Finally, the heat forming operation, dry-fit verification process, and core bond cycle were performed at 2.76×10^5 Pa. While the tests showed that 1.01×10^5 Pa and 2.76×10^5 Pa gave equivalent results, the actual UPS has more geometric complexity than what was simulated in the test matrix.

Core bond cycle observations: Although the flatwise tension test matrix presented could not differentiate between a one-step or two-step core bond process, the team observed poor handling strength of coupons after the first tack step was completed. Therefore, while the final strength was acceptable, damage could occur to the bond after the first tack step. Moreover, higher handling stresses were imposed during the layup of the OML than were required on flat panel layup. In addition to the lack of strength after the tack operation, the minimum viscosity achieved was influenced by several factors: the two-step process, slower than specified ramp rates, and an intermediate hold temperature. This increased minimum viscosity has the potential to make us more sensitive to core fit-up, because the filleting is reduced, decreasing the effective bond overlap.

Core bond cycle corrective actions: In order to achieve the maximum handling strength, the core-to-IML bond was taken to full cure in one-step. The original motivation for going to a tack bond process (two step was to reduce warping of the asymmetric configuration. However, this was mitigated by the fact that the UPS is of closed form geometry as opposed to a flat panel. In order to achieve the lowest viscosity practical for core bonding, the 180°F intermediate hold was removed. However, this was a moisture removal step. Therefore, a room temperature, 8 hour minimum, debulk step was added to mitigate the moisture concern, without compromising the minimum viscosity. In addition, manufacturing controls were adjusted to ensure that the specified and validated ramp rate of $0.55^\circ\text{C}/\text{min}$ could be achieved, which was not achieved on the demonstration article.

Along with these major corrective actions, some minor best-practice changes were made. These include switching film adhesive carrier types on the precured side from M (mat) to K (knit), while retaining the M carrier on the co-cured side. The K allows for better adhesive flow on the

pre-cured side, whereas the M minimizes dimpling on the co-cured side. In addition, a pin roller was used on the film adhesive to facilitate air removal. From a design perspective, the number of hatch plies was increased from 1 to 4, in order to reduce the risk of water penetration during ultrasonic inspection and decrease the number of ply drops. Finally, a previous lesson learned on thin shell buckling during autoclave pressurization was brought to the team's attention. This reference led the team to pressurize at 104 °C rather than room temperature, during both the core forming and core bonding, to reduce the IML buckling risk. All of the corrective actions were demonstrated on a curved process validation article, described in Reference 4.

7. CONCLUSIONS

Several process anomalies were encountered during the development of the CCM. They include, a splice re-design, pi preform consolidation defects, and a disbond of the inner skin-to-core, which was the focus of this paper. While process development and associated building block testing were performed in each of these areas, the anomalies manifested themselves at the full-scale level due to interactions between process robustness and manufacturing scale-up. This highlights the importance of full-scale developmental work early in the development phase of a composite project.

8. REFERENCES

1. Kirsch, Michael T. *Composite Crew Module: Primary Structure*. NASA/TM-2011-217185, NESC-RP-06-019. November 2011.
2. Watson, Dave. *Composite Crew Module: Design*. NESC-RP-06-019. November 2011. Also published as NASA/TM-2011-217186.
3. Jeans, James W. *Composite Crew Module: Analysis*. NESC-RP-06-019. November 2011. also published as NASA/TM-2011-217188.
4. Polis, Daniel L. *Composite Crew Module: Materials and Processes*. NESC-RP-06-019. November 2011. Also published as NASA/TM-2011-217187.
5. Pelham, Larry. *Composite Crew Module: Manufacturing*. NESC-RP-06-019. November 2011. Also published as NASA/TM-2011-217189.
6. Hodges, Kenneth L. *Composite Crew Module: Nondestructive Evaluation Report*. NESC-RP-06-019. November 2011. Also published as NASA/TM-2011-217191.
7. Kellas, Sotiris. *Composite Crew Module: Test*. NESC-RP-06-019. November 2011. Also published as NASA/TM-2011-217190.
8. T. Curiel, G. Fernlund / *Composites: Part A* 39 (2008) 252–261.
9. ASTM C297, Standard Test Method for Flatwise Tensile Strength of Sandwich Constructions.

9. ACKNOWLEDGEMENT

The author would like to give special thanks to Mr. Larry Pelham (NASA/MSFC) and Mr. Dawson Vincent (NG), who led the test panel fabrication for this study, Dr. Allen Nettles (NASA/MSFC) who provided photomicrographs of the core filleting, and Dr. Tan-Hung Hou (NASA/LaRC) for his rheological support. Additional thanks to the entire CCM team for their contributions toward this work and all of the other materials and process activities.